DOI: 10.1534/genetics.107.082149

Gene Expression Profiling of Flagellar Disassembly in *Chlamydomonas reinhardtii*

Kara L. Chamberlain, Steven H. Miller and Laura R. Keller[1]

Department of Biological Science, Florida State University, Tallahassee, Florida 32306-4370

Manuscript received September 21, 2007
Accepted for publication December 6, 2007

ABSTRACT

Flagella are sensory organelles that interact with the environment through signal transduction and gene expression networks. We used microarray profiling to examine gene regulation associated with flagellar length change in the green alga *Chlamydomonas reinhardtii*. Microarrays were probed with fluorescently labeled cDNAs synthesized from RNA extracted from cells before and during flagellar assembly or disassembly. Evaluation of the gene expression profiles identified >100 clones showing at least a twofold change in expression during flagellar length changes. Products of these genes are associated not only with flagellar structure and motility but also with other cellular responses, including signal transduction and metabolism. Expression of specific genes from each category was further characterized at higher resolution by using quantitative real-time PCR (qRT–PCR). Analysis and comparison of the gene expression profiles coupled to flagellar assembly and disassembly revealed that each process involves a new and uncharacterized whole-cell response to flagellar length changes. This analysis lays the groundwork for a more comprehensive understanding of the cellular and molecular networks regulating flagellar length changes.

CELLS monitor and respond to changes in the environment through tight coordination of signal transduction and gene expression networks. Cilia and flagella, similar complex organelles that receive and integrate extracellular signals, play a major role in mediating how a cell interacts with its environment (reviewed by Ainsworth 2007 and by Christensen *et al.* 2007). Recently, studies of such diverse model systems as *Chlamydomonas reinhardtii*, *Caenorhabditis elegans*, *Drosophila melanogaster*, and *Mus musculus* (reviewed by Davenport and Yoder 2005; Pan *et al.* 2005) have linked defects in ciliary structure and function directly to known human diseases such as polycystic kidney disease and Bardet–Biedl syndrome (Pazour *et al.* 2000, 2005; Li *et al.* 2004; Sun *et al.* 2004; Stolc *et al.* 2005). Identification of the components and mechanisms involved in flagellar structure and function has begun to elucidate the signal transduction networks, but the genes involved remain incompletely understood (Davenport and Yoder 2005).

The unicellular green alga *C. reinhardtii* provides an excellent model system for investigating flagellar gene expression network responses. It has two flagella that act as environmental sensors for the cell. Changing the cell's environment in various ways causes changes in flagellar morphology. For example, experimental acidification of the medium (acid shock) induces flagellar excision (Witman *et al.* 1972) followed by regrowth (hereafter referred to as assembly) of new flagella within 2 hr (Rosenbaum *et al.* 1969; Lefebvre *et al.* 1978). Stimulation with either isobutyl methylxanthine (IBMX) (Lefebvre *et al.* 1980) or sodium pyrophosphate (Lefebvre *et al.* 1978) induces resorption or shortening of the flagella (hereafter referred to as disassembly).

Many previous investigations have demonstrated coordination between flagellar gene expression and flagellar assembly. During the course of flagellar assembly, for example, genes encoding α- and β-tubulin are transiently upregulated and return to prestimulation levels as the regenerating flagella reach full length (Lefebvre *et al.* 1980; Silflow *et al.* 1982; Baker *et al.* 1984; Keller *et al.* 1984; Schloss *et al.* 1984). Recent genomic and proteomic studies by Stolc *et al.* (2005) and Pazour *et al.* (2005) have profiled similar expression patterns for large numbers of additional genes during flagellar assembly. Although the coordination of structure and gene expression is well characterized for flagellar assembly, known gene regulation during disassembly is largely limited to a decrease in expression of α- and β-tubulin mRNA levels (Lefebvre *et al.* 1980; Silflow *et al.* 1982).

An important aspect of understanding coordination of flagellar structure and function is identification of genes whose expression is regulated during flagellar assembly and disassembly. We used a genomics approach to identify *C. reinhardtii* genes showing changes in expression during flagellar disassembly. By evaluating a large gene set, we established an expression profile for flagellar disassembly. Furthermore, we compared the

[1]*Corresponding author:* Department of Biological Science, Florida State University, Tallahassee, FL 32306-4370. E-mail: lkeller@bio.fsu.edu.

expression profile for disassembly to that for assembly to determine whether common sets of genes are coordinately or differentially regulated. Because many structural genes are already characterized, uncovering genes associated with the regulatory mechanism was of particular interest. Evaluation of assembly and disassembly expression profiles provides a necessary step for defining the complex cellular and molecular networks involved in regulating flagellar length change.

MATERIALS AND METHODS

Cell culture: *C. reinhardtii* wild-type strain 137c^{-} (CC-124) (*Chlamydomonas* Center, http://www.chlamy.org) was cultured in medium I (Sager and Granick 1953) at 25° with continuous aeration on a 14:10-hr light:dark cycle. Before stimulation, cells were harvested by centrifugation (~4000 × *g*, 6 min) and then resuspended in a buffer containing 10 mm piperazine-*N*,*N*′-bis[2-ethanesulfonic acid]–potassium hydroxide (PIPES–KOH), pH 7.2, 500 μm $CaCl_2$. Cells recovered under fluorescent light at room temperature for 2 hr. To monitor cell viability and flagellar lengths, we fixed a cell sample in an equal volume of 2% glutaraldehyde and examined the sample by phase-contrast microscopy (Carl Zeiss, Thornwood, NY). Flagellar lengths were measured with an ocular micrometer.

Cell stimulation and total RNA extraction: For measurement of flagellar assembly, acetic acid (0.2 n) was added to the cell culture to lower the sample pH to <4.3 and then, after 30 sec, KOH (0.2 n) was added to return the sample to pH 7.2 (Evans and Keller 1997). This acid shock experimentally induced flagellar excision, which was followed by assembly. For measurement of disassembly, disassembly was experimentally stimulated by IBMX (Sigma, St. Louis). IBMX was dissolved in dimethyl sulfoxide (DMSO; Sigma) to a stock concentration of 200 mm. Cells were stimulated by addition of IBMX to a final concentration of 0.4 mm (Lefebvre *et al.* 1980). At 30, 60, and 90 min after stimulation, live cells were examined, and the percentages of deflagellation and flagellar length were determined on fixed cells. Total RNA was extracted before and at 30, 60, and 90 min after stimulation with the RNeasy mini kit (QIAGEN, Valencia, CA). The concentration of total RNA was determined by measurement of the A_{260}/A_{280} with UV spectrophotometry (NanoDrop, Wilmington, DE) and RNA integrity was assessed with guanidine thiocyanate denaturing gels. For each stimulus, total RNA at each time point was extracted on three different days.

Fabrication of microarray: *C. reinhardtii* cDNA clones were prepared from a cDNA library (*Chlamydomonas* Center, http://www.chlamy.org) cloned into a Stratagene (La Jolla, CA) Uni-ZAP mass excision vector system. This cDNA library was prepared from RNA isolated 15, 30, and 60 min after deflagellation by acid shock treatment. Plasmids were isolated with a 96-well vacuum manifold to produce 960 clones (Eppendorf, Westbury, NY, and Millipore, Billerica, MA). cDNA inserts from each clone were PCR amplified (Eppendorf Master Taq) with T3 and T7 primers in a 96-well format according to this protocol: 94° for 1 min; 30 cycles of 94° for 30 sec, 50° for 1 min, and 72° for 2 min; followed by an extension phase of 72° for 10 min. Every PCR reaction produced a single band on a 1% agarose gels. As controls, purified PCR products from α- and β-tubulins, radial spoke proteins (RSP3, RSP4, and RSP6), and pcf8-13 were included.

PCR products were suspended in 50% DMSO, which promotes hybridization (Hegde *et al.* 2000), and distributed into 384-well microtiter plates (Genetix, Boston) to a final concentration of 100 ng/μl (Yue *et al.* 2001). Arrays were printed with a 16-quill pin tool on the *Micro*Grid robot (BioRobotics, Cambridgeshire, UK) at a 0.4-mm pitch. In the custom spotting pattern, each sample was duplicated as a control for quality and variability across the slide (Yang and Speed 2002; Bowtell and Sambrook 2003). To ensure uniform spot morphology, we controlled temperature (20°–35°) and relative humidity (45–55%) levels throughout the array printing (Hegde *et al.* 2000). Purified PCR products were spotted onto Corning (Corning, NY) CMT-GAPS II slides, with an average spot diameter of 200 μm, and immobilized by baking at 80° for 5 hr (Corning CMT-GAPS II DMSO protocol). The printed slides were stored until use in a desiccator at room temperature.

Fluorescent labeling and hybridization: Total RNA (20 μg) was converted into first-strand cDNA with the SuperScript Indirect cDNA labeling system (Invitrogen, Carlsbad, CA). Immediately after cDNA synthesis, the original template was hydrolyzed and cDNA products purified with the S.N.A.P. column purification module (Invitrogen). The amino-allyl-modified cDNA from each time point was coupled to one of four different Alexa Fluor dyes (Invitrogen): Alexa Fluor 555 for untreated, Alexa Fluor 647 for 30 min, Alexa Fluor 594 for 60 min, and Alexa Fluor 488 for the 90-min time point. The microarray slides were prehybridized in 5× SSC (Fisher Scientific, Waltham, MA), 0.1% SDS (Sigma), and 25% formamide (Fisher Scientific) for 45 min at 42°; rinsed in distilled water; allowed to dry; and then placed in a hybridization chamber (ArrayIt, Telechem International, Sunnyvale, CA). Each microarray slide was then cohybridized with a mixture of the four Alexa-Fluor-labeled cDNAs at 42° for 18 hr in the dark. After hybridization, the slides were washed once in 1× SSC, 0.2% SDS, at 55° for 10 min; twice in 0.1× SSC, 0.2% SDS, at 55° for 10 min; twice in 0.1× SSC at room temperature for 1 min; and once in dH_2O at room temperature for 10 sec. (Amersham Biosciences protocol). The slides were allowed to dry and then laser scanned with the ScanArray 5000XL scanner (GSI Lumonics, Moorpark, CA). Labeling and hybridization for each time course were repeated three independent times.

Microarray data analysis: QuantArray imaging software (BD Biosciences, San Jose, CA) was used to quantify fluorophore intensity. Background intensity was subtracted from spot intensity by a fixed-circle segmentation method. The resulting data were exported, and GeneSifter web-based software (http://www.genesifter.net) normalized them (Global Adjust) to correct for systematic differences in the intensity of the channels (Bowtell and Sambrook 2003). Fold change for each time point was calculated by comparing to the untreated sample. Selection criteria for evaluation of expression included a pairwise comparison of biological and on-slide replicates as well as a cutoff of twofold or greater change in relative abundance. The clones that met these criteria were chosen for DNA sequencing and characterization by database searches at the Joint Genome Institute (JGI, http://genome.jgi-psf.org/Chlre3/Chlre3.home.html) and National Center for Biotechnology Information (NCBI, http://www.ncbi.nlm.nih.gov).

Quantitative real-time polymerase chain reaction: On the basis of the selection criterion outlined above, several genes showing differential expression were chosen for further analysis by quantitative real-time polymerase chain reaction (qRT–PCR). Primer sets with a melting temperature of 59°–60° and a product size between 90 and 150 bp were designed using Primer Quest (Integrated DNA Technologies, Coralville, IA, http://www.idtdna.com). Forward and reverse primer sets for each gene (Operon, Huntsville, AL; see supplemental Table 1 at http://www.genetics.org/supplemental/) were diluted to 10 μm and tested for a single product of the correct size with standard PCR and gel electrophoresis. The same total RNA

used for the microarray profiles was used for qRT–PCR. First-strand cDNA synthesis was performed with 2 μg total RNA from each time point according to the manufacturer's protocol (SuperScript first-strand synthesis system for RT–PCR, Invitrogen). cDNA diluted 20-fold was combined with primer pairs and SYBR Green PCR master mix (Applied Biosystems, Foster City, CA) on an Applied Biosystems 7500 Fast Real-Time PCR system (Foster City, CA) according to the following protocol: 50° for 2 min; 95° for 10 min; 40 cycles of 95° for 15 sec, 60° for 30 sec, 68° for 30 sec; followed by a dissociation cycle. For each biological repetition, qRT–PCR was performed on all genes, including technical replicates and nontemplate controls. For each gene, a common threshold setting applied to each of the three biological replicates determined the threshold cycle (C_T). Relative abundance of each gene was determined by the $2^{-\Delta\Delta Ct}$ method (Livak and Schmittgen 2001). pcf8-13 (Schloss 1990) was used as the endogenous control for calculation of relative abundance. Relative abundances for time points 30, 60, and 90 min after stimulation were then standardized to that for untreated cells. Fold change and standard error (SE) were log transformed for graphical representation.

RESULTS

Microarray construction and preliminary data analysis: We constructed our array using a cDNA library prepared from *C. reinhardtii* RNA isolated at 15, 30, and 60 min during flagellar assembly. The strategic use of the cDNA library that we used created an inherent bias in our analysis because known flagellar genes are induced during assembly, but it also increased the probability of identifying genes involved in the response to flagellar length change.

After experimentally induced flagellar excision, flagella assembled to ~80% of the length of those of untreated cells by 90 min (Figure 1). After experimental stimulation of disassembly, flagella disassembled to ~50% the length of those of untreated cells by 90 min (Figure 1). Control cells treated with DMSO, the solvent for IBMX, demonstrated no change in flagellar length (data not shown).

To assess differential gene expression over time, we extracted total RNA from cells before and at 30, 60, and 90 min following stimulation. Fluorescently labeled cDNAs synthesized from these RNAs were hybridized to the microarray. For each stimulus, the kinetics of how each gene responded was tracked over time through changes in relative abundance. The signal intensity at each time point compared to that of untreated cells reflects relative mRNA abundance. For each gene studied, the collective data from three independent experiments are visually represented in a heat map (Table 1) in which upregulation is represented in red, downregulation in green, and no change in black. Analysis of the 960 unique clones revealed that 118 showed a change in intensity of twofold or greater (Table 1). These 118 clones were sequenced and characterized by means of JGI and NCBI database searches; genes showing less than a twofold change in intensity were not characterized further. The constitutively expressed pcf8-13 gene was included as a control. The expression patterns of the genes selected for characterization are described below.

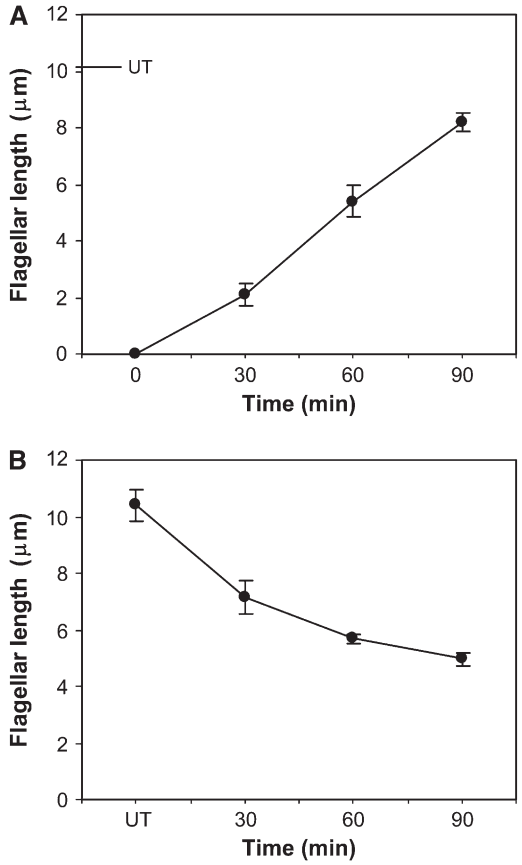

Figure 1.—Changes in flagellar length during acid shock and IBMX-induced flagellar assembly and disassembly. Flagellar lengths were measured with an ocular micrometer before and 30, 60, and 90 min after stimulation. Data are the arithmetic means and standard deviations of the length measurements. (A) Cells were stimulated by acid shock, which induced flagellar excision followed by assembly. UT (untreated) is prestimulation flagellar length. (B) Cells were stimulated with 0.4 mM IBMX, which induced flagellar disassembly.

Microarray expression profiling of flagellar assembly and disassembly: Our genomic expression profiling uncovered differential expression of several genes involved in the cellular response to flagellar assembly and disassembly. We organized these genes into four eukaryotic orthologous groups (KOG): cellular processes and signaling, information storage and processing, metabolism, and poorly characterized genes (Table 1). Within each category, genes were subcategorized on the basis of their cellular or molecular functions. Figure 2 displays the distribution in each subcategory. The largest groups included cell motility (13%), energy production and conversion (17%), and signal transduction mechanisms (18%).

The levels of α- and β-tubulin mRNA abundance increased after acid shock (Table 1), confirming previous studies of α- and β-tubulin expression during

TABLE 1

Gene identification and expression profiles of selected genes

Name	Description	NCBI accession no.	JGI v3.0 gene model name ID	Microarray heat map[a] (−2 0 2) Acid shock (assembly) 0′	30′	60′	90′	IBMX (disassembly) 0′	30′	60′	90′
Cellular processes and signaling											
	Cell motility										
DHC1[b,c]	Dynein heavy chain 1 α (PF9)	AJ243806.1	estExt_GenewiseH_1.C_880001								
DLC7b[c]	LC7b, similar to the Roadblock/LC7 family	AY457969	SAN_chlre3.20.7.3.11								
IFT52[b,c]	Intraflagellar transport 52 (BLD1)	AF420244	estExt_fgenesh1_pm.C_150001								
PF16[c]	Central pair-associated protein	U40057	e_gwH.23.36.1								
RSP3[b,c]	Radial spoke protein 3	X14549	estExt_gwp_1W.C_260138								
RSP4[b,c]	Radial spoke protein 4	M87526	estExt_fgenesh1_pm.C_60005								
RSP6[b,c]	Radial spoke protein 6	M87526	estExt_GenewiseH_1.C_60055								
TUA1[b,c]	α-Tubulin 1	M11447	estExt_gwp_1H.C_140050								
TUA2[c]	α-Tubulin 2	M11448	estExt_fgenesh2_kg.C_860004								
TUB1[b,c,d]	β-Tubulin 1	M10064	estExt_gwp_1H.C_200099								
TUB2[b,c,d]	β-Tubulin 2	K03281	estExt_gwp_1H.C_200090								
VFL2[b,c]	Centrin (caltractin)	X57973	acegs_kg.scaffold_48000029								
	Post-translational modification, protein turnover, chaperones										
HSP22A	Heat-shock protein 22A	X15053	estExt_gwp_1W.C_60086								
HSP22B	Heat-shock protein 22B		Chlre2_kg.scaffold_6000241								
HSP22D	Heat-shock protein 22D		estExt_fgenesh2_pg.C_10198								
HSP90A	Heat-shock protein 90A, localized to cytosol		estExt_gwp_1W.C_250014								
HSP90C	Heat-shock protein 90C, localized to chloroplast	AY705371	Chlre2_kg.scaffold_83000033								
FAP277[c]	Flagellar-associated protein, protease inhibitor		SKA_Chlre2_kg.scaffold_28000189								
LF4[c]	Long flagella protein	AY231293	Chlre2_kg.scaffold_2000376								
—[e]	Tyrosine-specific protein phosphatase		estExt_fgenesh2_pg.C_60262								
—[e]	Unknown: AMPKbeta_GBD_like		fgenesh2_kg.C_scaffold_22000004								
	Signal transduction mechanisms										
CRT2	Calreticulin 2	AJ000765	estExt_GenewiseW_1.C_10142								
FAP12[c]	Flagellar-associated, lipase domain (pcf3-21)		estExt_fgenesh2_kg.C_240073								
—[e]	G-protein-coupled seven transmembrane receptor		estExt_gwp_1H.C_310074								
—[d,e]	GPR1/FUN34/yaaH, five transmembrane domains		e_gwH.13.239.1								
—[e]	GPR1/FUN34/yaaH, six transmembrane domains		estExt_gwp_1W.C_130172								
GUN4	Similar to Gun4 (genomes uncoupled 4)		SKA_estExt_fgenesh2_pg.C_60106								
MIPS[d]	*Myo*-inositol-1-phosphate synthase		estExt_fgenesh2_pg.C_90007								
NDA3[b]	Putative mitochondrial NADH dehydrogenase		PIE_e_gwH.76.22.1								
—[d,e]	Putative membrane protein, five transmembrane domains		estExt_fgenesh2_pg.C_20320								
RACK1[b]	Receptor of activated protein kinase C 1 (pcf8-13)		e_gwH.38.29.1								
—[d,e]	Thylakoid membrane protein, PGR5-like		estExt_gwp_1H.C_60062								
	Intracellular trafficking, secretion, vesicular transport										
ARFA1a[c]	Small Arf-related GTPase	U27120	estExt_fgenesh2_kg.C_110094								
RABE1	Small Rab-related GTPase		SAN_163210								

(*continued*)

TABLE 1

(Continued)

Name	Description	NCBI accession no.	JGI v3.0 gene model name ID	Microarray heat map[a] Acid shock (assembly) 0′	30′	60′	90′	IBMX (disassembly) 0′	30′	60′	90′
Information storage and processing											
	Translation, ribosomal structure, and biogenesis										
IF4A[c]	Putative eukaryotic IF4A subunit (EIF41)		estExt_fgenesh2_pg.C_120244								
MTT1	Mitochondrial transcription termination factor like		estExt_fgenesh2_kg.C_390018								
NOP56	Nucleolar protein, component of C/D snoRNPs		estExt_gwp_1H.C_310180								
PRPL7/L12	Chloroplast ribosomal protein L7/L12		e_gwH.2.436.1								
RPL13	Ribosomal protein L13		estExt_gwp_1H.C_170118								
RPL15	Ribosomal protein L15		estExt_GenewiseW_1.C_70201								
RPL17	Ribosomal protein L17		estExt_GenewiseW_1.C_20197								
RPL23a	Ribosomal protein L23a		fgenesh2_pg.C_scaffold_26000093								
RPL27a	Ribosomal protein L27a		acegs_kg.scaffold_5000022								
RPS16	Ribosomal protein S16		MAY_e_gwW.2.213.1								
RPS19	Ribosomal protein S19		Chlre2_kg.scaffold_5000208								
RPS3a	Ribosomal protein S3a		fgenesh2_pg.C_scaffold_2000130								
—[e]	Small subunit ribosomal RNA-18S rDNA	M32703	estExt_gwp_1H.C_4800003[f]								
	Transcription										
FAP280[c,d]	Flagellar-associated, transcriptional coactivator-like		estExt_GenewiseW_1.C_50164								
—[d,e]	Putative zinc-finger protein, A20-like and AN1-like		OVA_e_gwH.25.97.1								
—[e]	Putative zinc-finger domain, RING		Chlre2_kg.scaffold_11000031								
Metabolism											
	Energy production and conversion										
ANT1[d]	Adenine nucleotide translocator 1	X65194	JLM_estExt_gwp_1W.C_250131								
COX2b	Cytochrome c oxidase subunit IIb (2b)	AF305540	estExt_fgenesh2_pg.C_10741								
CYB5_1	Putative cytochrome b5 protein		estExt_gwp_1H.C_370036								
GRX3	Glutaredoxin 3, CGFS type, probably chloroplastic		estExt_fgenesh2_pg.C_810010								
ICL1[c]	Isocitrate lyase	U18765	estExt_fgenesh2_pg.C_260094								
LHCA2	Light-harvesting protein of photosystem I		Chlre2_kg.scaffold_11000154								
LHCA5	Light-harvesting protein of photosystem I	DQ370095	estExt_fgenesh2_pg.C_80188								
LHCB5	Minor chlorophyll a-b-binding protein of PSII (CP26)	AB050007	estExt_fgenesh2_kg.C_280035								
LHCBM2[d]	Light-harvesting complex II chlorophyll a-b binding	AB051205	estExt_fgenesh2_kg.C_200058								
LHCBM3[d]	Light-harvesting complex II chlorophyll a-b binding M3	AB051208	estExt_fgenesh2_pg.C_940011								
LHCBM9[d]	Light-harvesting complex II chlorophyll a-b binding	AF495472	estExt_fgenesh2_kg.C_260046[g]								
PSAH	Subunit H of photosystem I (protein P28)	X15164	estExt_fgenesh2_kg.C_100106								
PSAI	Photosystem I subunit VIII, chloroplast-targeted		Chlre2_kg.scaffold_9000287								
PTOX2	Putative plastid terminal oxidase	AF494290	SKA_estExt_fgenesh2_pg.C_90141								
	Amino acid transport and metabolism										
—[e]	Asp/Glu racemase		estExt_fgenesh2_kg.C_10277								
HPD2	4-Hydroxyphenylpyruvate dioxygenase	AJ431261	Chlre2_kg.scaffold_23000178								

(*continued*)

TABLE 1

(Continued)

Name	Description	NCBI accession no.	JGI v3.0 gene model name ID	Microarray heat map[a] (−2 0 2) Acid shock (assembly) 0′	30′	60′	90′	IBMX (disassembly) 0′	30′	60′	90′
	Carbohydrate transport and metabolism										
PFK2	Phosphofructokinase family (EC 2.7.1.11 or 2.7.1.90)		MHS_estExt_gwp_1W.C_200088								
RBCS2B	RuBisCO small subunit 2	X04472	estExt_GenewiseH_1.C_790027								
UPTG1	UDP-glucose:protein transglucosylase		estExt_fgenesh2_pg.C_20070								
	Coenzyme transport and metabolism										
PDX1	Pyridoxin biosynthesis protein		estExt_fgenesh2_pg.C_590022								
	Lipid transport and metabolism										
SPT1	Serine palmitoyltransferase		e_gwW.15.128.1								
	Ion transport and metabolism										
ATS1	ATP-sulfurylase	U57088	HAL_estExt_fgenesh2_kg.C_190083								
COP3[d]	Light-gated proton channel rhodopsin	AF508967	Chlre2_kg.scaffold_43000011								
	Secondary metabolite biosynthesis, transport, and catabolism										
HDS	1-Hydroxy-2-methyl-2-(E)-butenyl4-diphosphate synthase	AY860817	estExt_GenewiseH_1.C_110006								
LAO1	L-Amino acid oxidase	U78797	estExt_fgenesh2_kg.C_200072								
Poorly characterized											
	General function prediction only										
CP12	Small polypeptide associating with GAPDH and PRK		Chlre2_kg.scaffold_21000100								
FAP294[c]	Flagellar-associated coiled-coil protein		estExt_fgenesh2_pg.C_250096								
FTT[c]	Fourteen-three-three, 14-3-3-like protein GF14 nu	X79445	estExt_fgenesh2_kg.C_800003								
LCI12	Low-CO2-inducible protein		acegs_kg.scaffold_389000001								
SMT1	Similar to sterol-C24-methyltransferase		fgenesh2_kg.C_scaffold_11000008								
ULP1	Uncharacterized lumenal polypeptide	X96877	estExt_fgenesh2_pg.C_10774								
—[e]	Unknown, patatin domain		Chlre2_kg.scaffold_19000064								
	Function unknown										
—[e]	Unknown		fgenesh2_pg.C_scaffold_60000034								
—[e]	Unknown		estExt_fgenesh2_kg.C_710007								
—[e]	Unknown		estExt_fgenesh2_pg.C_230120								
—[e]	Unknown		estExt_fgenesh2_pg.C_20470								
—[e]	Unknown, three transmembrane domains		estExt_fgenesh2_kg.C_70077								
—[e]	Unknown, eight transmembrane domains		Chlre2_kg.scaffold_12000168								
—[e]	Unknown		OVA_Chlre2_kg.scaffold_21000142								
			Chlre2_kg.scaffold_8000021[f]								
—[e]	Unknown, phosphoprotein-like		Chlre2_kg.scaffold_124000001								

Clones (118) sequenced and characterized by JGI and NCBI database searches were grouped into eukaryotic orthologous groups. Heat maps show relative mRNA abundance at each time point compared to that of untreated cells. Upregulation is represented in red, downregulation in green, and no change in black.

[a] Heat maps generated using GeneSifter represent the collective data from three independent experiments.

[b] PCR products were included on microarray for control purposes.

[c] Found in the flagellar proteome according to Pazour *et al.* (2005) and/or JGI.

[d] Genes represent more than one clone on microarray.

[e] Genes not yet named.

[f] Maps to multiple scaffolds on JGI.

[g] Also maps on JGI to LHCBM4 (estExt_fgenesh2_pg.C_260118) and to LHCBM6 (estEXT_fgenesh2_kg.C_260057).

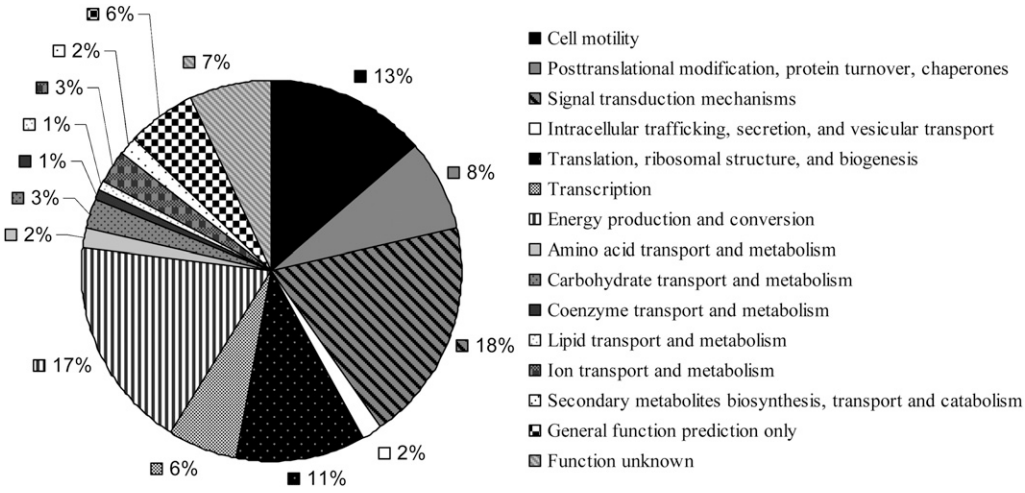

Figure 2.—Distribution into eukaryotic orthologous groups of the 118 clones on the microarray whose mRNAs exhibited at least a twofold change in abundance. Also included is the RACK1 clone, which showed no differential expression. Categories listed in the key correspond to sectors of the graph shown clockwise from the top. The largest eukaryotic orthologous groups included cell motility (13%), energy production and conversion (17%), and signal transduction mechanisms (18%).

flagellar assembly (Lefebvre *et al.* 1980; Silflow *et al.* 1982; Baker *et al.* 1984; Cheshire *et al.* 1994; Schloss *et al.* 1984; Evans and Keller 1997; Stolc *et al.* 2005). In contrast, the abundance of α- and β-tubulin mRNA decreased during flagellar disassembly (Table 1), confirming previous *in vitro* translation studies (Lefebvre *et al.* 1980; Silflow *et al.* 1982).

We also extended the expression profile of disassembly to include other structural components of the flagellum. For example, cell motility genes (including but not limited to structural genes of the flagellum) encoding radial spoke proteins; the central pair-associated protein PF16; and DLC7b, a member of the LC7/Roadblock family of dynein light chains, demonstrated downregulation during flagellar disassembly (Table 1). Genes in several other gene categories—for example, signal transduction genes, such as calreticulin (CRT) and myo-inositol-1-phosphate synthase (MIPS), and several transmembrane receptors—also displayed mRNA abundance decreases during flagellar disassembly (Table 1).

Genes in other categories showed different expression patterns. For example, genes encoding components of the light-harvesting complex (LHC) showed a similar downregulation of expression during both assembly and disassembly (Table 1). In contrast, genes encoding the heat-shock proteins (HSPs) 22B, 22D, and 90C each showed a unique expression pattern (Table 1). These genes have not previously been associated with flagellar structure or function, so this result suggests a new potential expression network associated with changes in flagellar length.

qRT–PCR expression profiling of selected genes: We selected several genes from various categories that demonstrated differential regulation in the microarray assay for characterization at higher resolution by qRT–PCR. The Chlamydomonas β-subunit-like polypeptide (CβLP/pcf8-13) (Schloss 1990) was used as an endogenous control because it is constitutively expressed during flagellar assembly as shown here in Figure 3A and previously (Schloss *et al.* 1984; Schloss 1990; Cheshire *et al.* 1994; Evans and Keller 1997). Sequence analysis revealed that pcf8-13 (CβLP) is RACK1, a receptor of activated protein kinase C 1 (data not shown). RACK1 was constitutively expressed throughout the time course of flagellar disassembly (Figure 3A).

Cellular processes and signaling—cell motility: We chose the well-characterized structural genes α- and β-tubulin for further analysis with qRT–PCR. Because of sequence similarity in the genes encoding the two α-tubulins (Silflow *et al.* 1985) and two β-tubulins (Youngblom *et al.* 1984), the relative mRNA abundance changes represent the contribution of both genes for each tubulin. As expected, the transcript levels of α- and β-tubulin increased during flagellar assembly and conversely decreased during disassembly, but the relative changes in α- and β-tubulin mRNA abundance were greater during disassembly (Figure 3, B and C). In addition, β-tubulin mRNA abundance was greater than that of α-tubulin during both assembly and disassembly (Figure 3, B and C).

To expand the expression profile of structural genes during flagellar disassembly, we assessed the relative levels of radial spoke protein (RSP) mRNAs. Radial spoke proteins form a structural complex in the flagellum essential for motility as well as signal transduction (Yang *et al.* 2006). mRNAs encoding RSP3, a component of the radial spoke stalk (Luck *et al.* 1977; Williams *et al.* 1989; Diener *et al.* 1993), and RSP4 and RSP6, components of the radial spoke head, showed increased abundance during assembly in previous studies (Williams *et al.* 1986; Curry *et al.* 1992). We demonstrated that, after IBMX treatment, RSP3, RSP4, and RSP6 mRNA abundances decreased during flagellar disassembly (Figure 3, D, E, and F). In both acid shock and IBMX, the kinetics of RSP3 expression differed somewhat from those of RSP4 and RSP6. By 30 min, RSP3 reached its maximal change in mRNA abundance and then declined (Figure 3D). In contrast, RSP4 and RSP6 transcripts were maximally expressed later in the time course at 60 min (Figure 3, E and F).

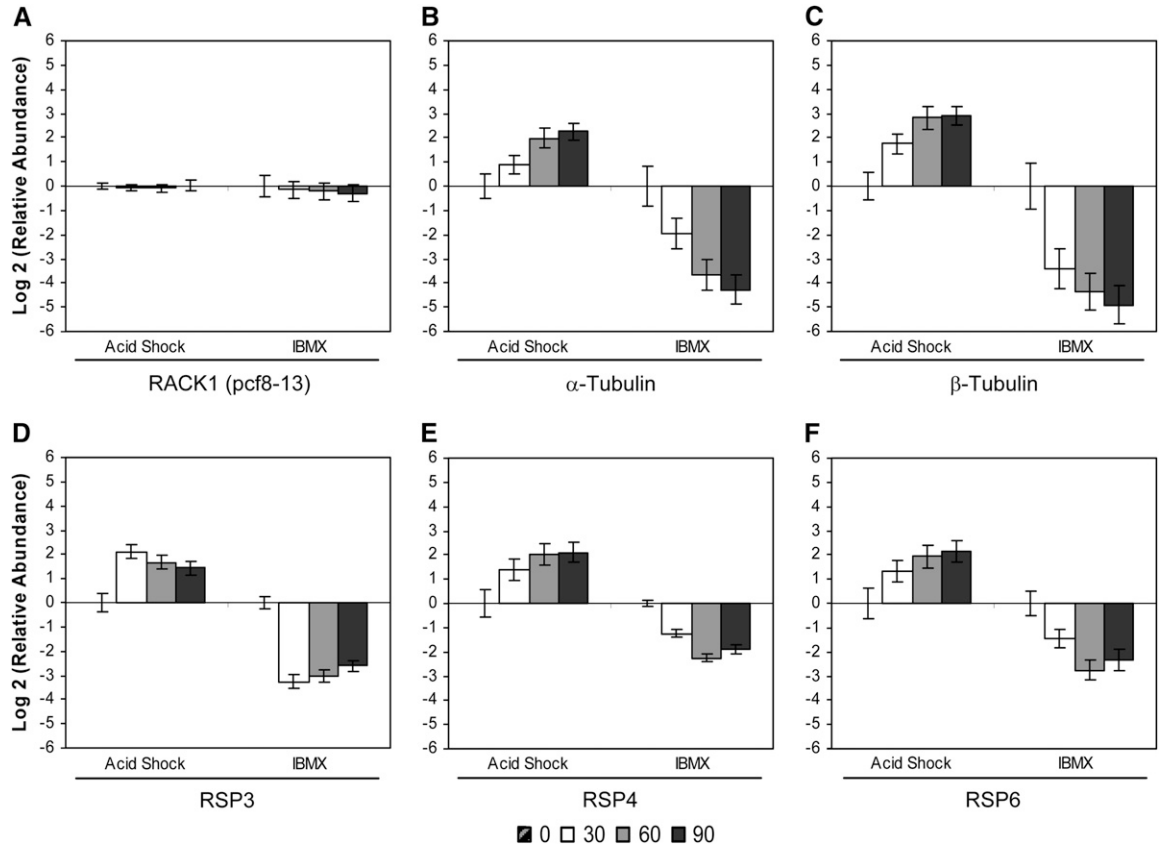

Figure 3.—Change in relative mRNA abundance of cell-motility genes during flagellar assembly (acid shock) and disassembly (IBMX) as measured by qRT–PCR. Relative abundance for each gene was determined by the $2^{-\Delta\Delta Ct}$ method. Fold change and standard error were log transformed for graphical representation. (A) RACK1 (pcf8-13) showed no change in relative mRNA abundance during flagellar assembly or disassembly and was used as the endogenous control for calculation of relative abundance. Changes in relative mRNA abundance for time points 30, 60, and 90 min after stimulation, standardized to untreated cells, were determined for (B) α-tubulin, (C) β-tubulin, (D) RSP3, (E) RSP4, and (F) RSP6.

Because the RSP4 and RSP6 genes encode components of the same complex, the similarity of their expression profiles is reasonable.

Flagellar-associated genes: We profiled expression of several less well-characterized genes recently shown to be present in the flagellar proteome (Pazour *et al.* 2005). FAP12, a partially characterized flagellar-associated protein with a lipase domain, was downregulated during flagellar disassembly to a greater degree than it was upregulated during assembly (Figure 4A). In our study, FAP12 mRNA reached its maximal abundance 90 min after either stimulation. We also found that FAP12 and pcf3-21, characterized in a previous study (Schloss *et al.* 1984), are encoded by the same gene (data not shown). In accordance with previous work (Schloss *et al.* 1984; Evans and Keller 1997; supplemental data for Pazour *et al.* 2005), the FAP12 (pcf3-21) gene was strongly upregulated during flagellar assembly and showed an expression profile similar to those of the major flagellar structural components.

Two other flagellar associated genes, FAP277 and FAP280, each showed a unique pattern of expression (Figure 4, B and C) and are thus exceptions to the characteristic profile of upregulation during assembly and downregulation during disassembly. The FAP277 gene was upregulated during both disassembly and assembly, but the magnitude of the mRNA abundance change during disassembly was less than half that during assembly (Figure 4B). In addition, a distinct increase in relative abundance occurred between 30 and 60 min during assembly but was not evident during disassembly. The FAP280 gene exhibited a more complex pattern. Its abundance was slightly increased 30 min into flagellar disassembly but returned to baseline by 60 min and then decreased by 90 min (Figure 4C). Therefore, not all genes associated with the flagellar proteome show the coordinated pattern of abundance upregulation during assembly and downregulation during disassembly.

Intraflagellar transport (IFT) plays important roles in flagellar assembly and disassembly. It transports flagellar components along the length of the axoneme (reviewed by Scholey 2003) and may act to regulate length (Marshall and Rosenbaum 2001; Marshall *et al.* 2005). IFT52 (BLD1/osm-6), an essential component for flagellar assembly (Brazelton *et al.* 2001), has been localized predominately around the basal body in

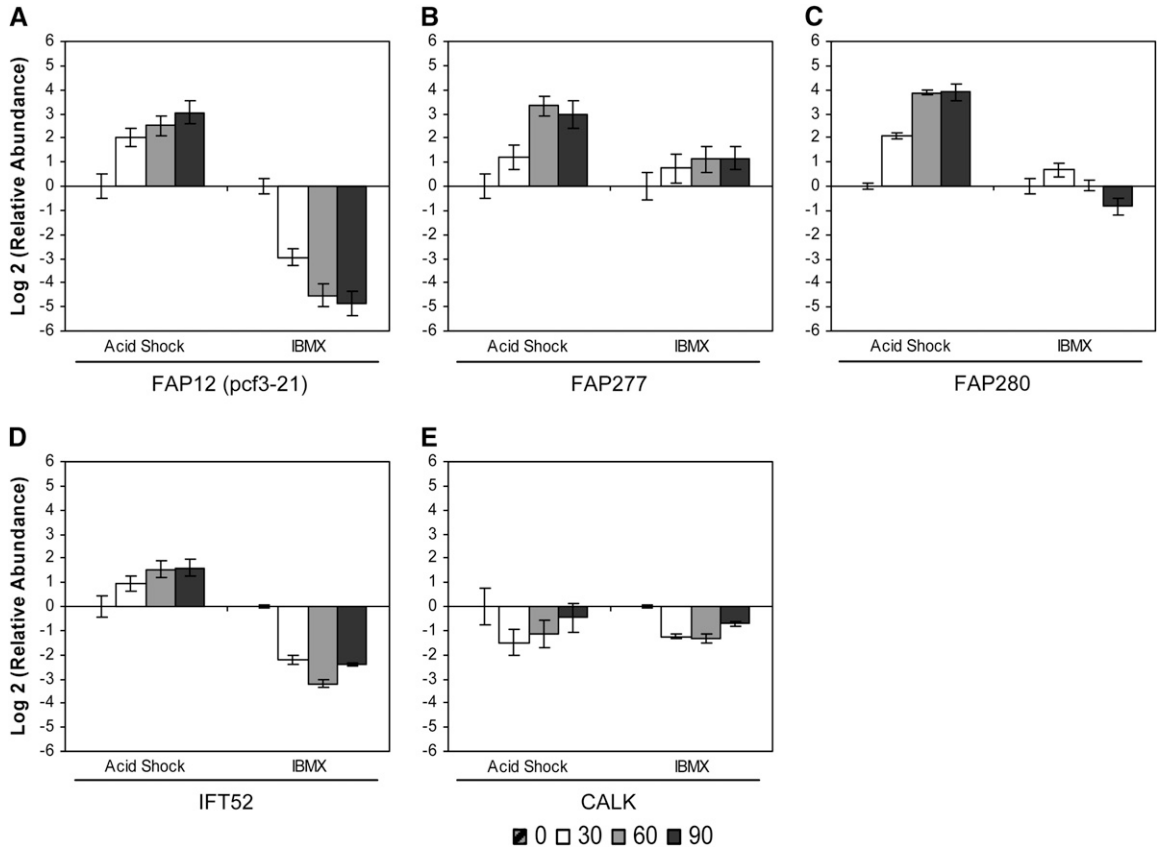

FIGURE 4.—Change in relative mRNA abundance of flagellar-associated genes during flagellar assembly (acid shock) and disassembly (IBMX) as measured by qRT–PCR. Relative abundance for each gene was determined by the $2^{-\Delta\Delta Ct}$ method. Fold change and standard error were log transformed for graphical representation. Changes in relative mRNA abundance for time points 30, 60, and 90 min after stimulation, standardized to untreated cells, were determined for (A) FAP12, (B) FAP277, (C) FAP280, (D) IFT52, and (E) CALK.

two horseshoe-shaped rings (DEANE *et al.* 2001). We found that the IFT52 gene was downregulated maximally at 60 min during disassembly (Figure 4D). In contrast, it was upregulated during assembly and maintained elevated expression as flagella reached pretreatment lengths (Figure 4D). We have therefore confirmed earlier reports of the abundance increase of IFT52 mRNA after flagellar loss (BRAZELTON *et al.* 2001; STOLC *et al.* 2005) and have extended the expression profile to include the 60- and 90-min time points (Figure 4D).

CALK, a Chlamydomonas aurora kinase, is a crucial element in the cell's ability to regulate flagellar excision and disassembly (PAN *et al.* 2004). CALK mRNA abundance decreased at 30 min in both assembly and disassembly but returned to near-pretreatment levels at 90 min (Figure 4E). PAN *et al.* (2004) demonstrated that the CALK protein acts in an early step in both flagellar loss and disassembly, so its downregulation is correlated with downregulation of its activity later in both assembly and disassembly.

Cellular processes and signaling—intracellular trafficking: We also found effects on expression of genes whose products are involved in a variety of other cellular activities beyond an association with flagellar function. Members of the ARF (ADP-ribosylation factor) family function in membrane trafficking (NIE and RANDAZZO 2006) and have known homologs linked to human ciliary disease. In *C. reinhardtii*, ARFA1a mRNA abundance decreased slightly during flagellar disassembly (Figure 5A), but during assembly, the relative abundance of ARFA1a mRNA clearly increased (Figure 5A). ARFA1a mRNA abundance reached its maximal at 60 min into flagellar assembly and then began to decline by 90 min (Figure 5A).

Cellular processes and signaling—signal transduction mechanisms: Previous work from our lab has demonstrated that the processes of flagellar excision, gene induction, and outgrowth are each independently regulated by calcium (Ca^{2+}) (CHESHIRE and KELLER 1991; CHESHIRE *et al.* 1994). Calreticulin (CRT2) is a calcium-binding protein localized to the endoplasmic/sarcoplasmic reticulum (reviewed by MICHALAK *et al.* 1992). The relative abundance of CRT2 mRNA decreased by 30 min into flagellar disassembly and then plateaued throughout the remainder of the time course (Figure 5B). In contrast, the relative abundance of CRT2 mRNA steadily increased to a peak at 90 min during assembly (Figure 5B).

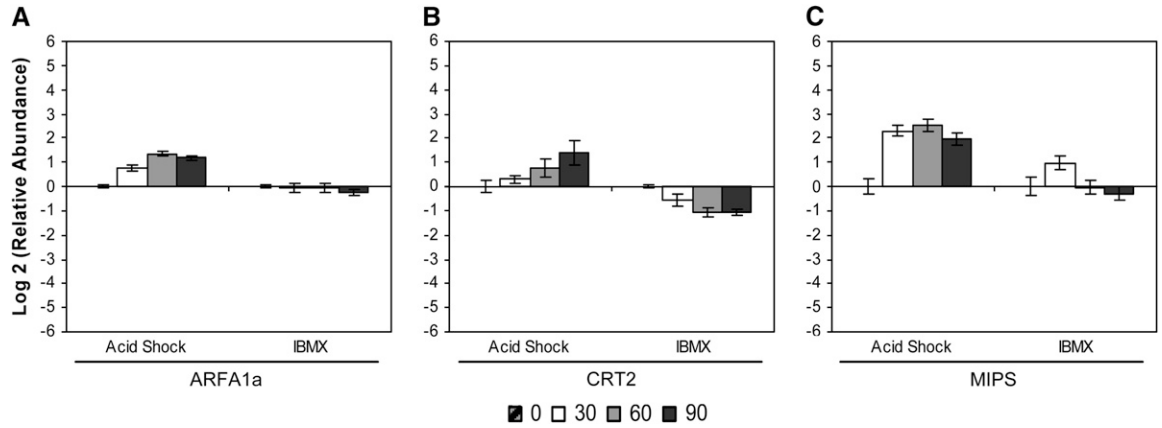

FIGURE 5.—Change in relative mRNA abundance of cellular processes and signaling genes during flagellar assembly (acid shock) and disassembly (IBMX) as measured by qRT–PCR. Relative abundance for each gene was determined by the $2^{-\Delta\Delta C_t}$ method. Fold change and standard error were log transformed for graphical representation. Changes in relative mRNA abundance for time points 30, 60, and 90 min after stimulation, standardized to untreated cells, were determined for (A) small ARF-related GTPase (ARFA1a), (B) CRT2, and (C) MIPS.

The gene encoding MIPS (EC 5.5.1.4), the first enzyme in the biosynthesis of inositol (MAJUMDER *et al.* 2003), exhibited a unique pattern of mRNA abundance during flagellar assembly and disassembly. During disassembly, the relative abundance of MIPS mRNA increased at 30 min but then was downregulated to pretreatment levels by 60 and 90 min (Figure 5C). In contrast, during flagellar assembly, MIPS mRNA abundance increased by 30 min, peaked, and then had begun to decline at 90 min (Figure 5C).

Metabolism—energy production and conversion: Several metabolism-related genes displayed similar expression profiles during both assembly and disassembly of the flagellum. The abundance of mRNA encoding isocitrate lyase (ICL1; EC 4.1.3.1), an enzyme in the glyoxylate pathway, increased after both acid shock and IBMX treatment (Figure 6A), whereas mRNAs encoding components of the photosynthetic apparatus decreased (Figure 6, B–D). The abundance of Lhca2 and Lhca5 mRNAs, encoding polypeptides of photosystem I (ELRAD and GROSSMAN 2004), showed similar decreases (Figure 6, B and C). Expression of Lhcb5 mRNA, encoding CP26 of the minor chlorophyll a-b binding protein of photosystem II (MINAGAWA *et al.* 2001; ELRAD and GROSSMAN 2004), decreased to a greater magnitude than that of Lhca2 and Lhca5 (Figure 6D). The expression profiles of the LHC genes therefore reveal coregulation of the individual components and suggest a common regulatory mechanism in response to external stimuli.

DISCUSSION

Microarray technology is generally agreed to be a valuable tool for high-throughput, parallel analysis of gene expression changes. Our custom microarray assay identified >100 clones showing distinct expression patterns. The products of these genes participate in activities such as cell motility, signal transduction, intracellular trafficking, and metabolism. Through characterization of these clones, we have established a global expression profile for flagellar disassembly.

As expected, we found expression of genes encoding major flagellar components during assembly, in accordance with many previous studies (LEFEBVRE *et al.* 1980; SILFLOW *et al.* 1982; BAKER *et al.* 1984; KELLER *et al.* 1984; SCHLOSS *et al.* 1984). In addition, our comparison of assembly and disassembly expression profiles for known flagellar genes (Table 1) reveals an overall trend of increased expression during flagellar assembly and decreased expression during disassembly. Thus, our study has expanded the expression profile of disassembly to include other genes encoding structural components of the flagellum and has established a coordination between changes in gene expression and changes in flagellar length.

The flagellar proteome consists of known structural proteins, as well as less well-characterized signal transduction proteins and flagellar associated proteins (FAPs) (PAZOUR *et al.* 2005). The genes encoding some FAPs show regulation during assembly (SCHLOSS *et al.* 1984; PAZOUR *et al.* 2005; STOLC *et al.* 2005), but whether these genes are regulated also during disassembly had not been explored before the study reported here. Among the genes we found to show regulation during assembly and disassembly are 21 whose products were identified by PAZOUR *et al.* (2005) as part of the flagellar proteome. For example, the expression profile of FAP12 is similar to that of known flagellar structural components. Alternatively, genes encoding the less well-characterized FAP277 and FAP280 exhibited unique regulation profiles that are not characteristic of known flagellar structural genes. Microarray technology has the ability to predict genes involved in regulatory

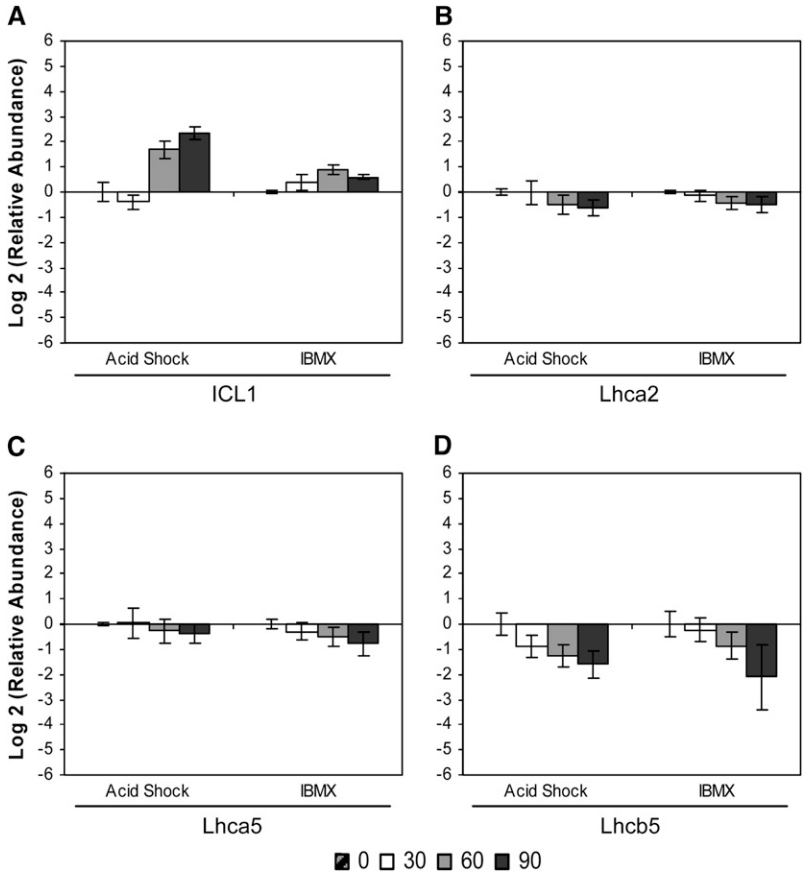

FIGURE 6.—Change in relative mRNA abundance of metabolism-related genes during flagellar assembly (acid shock) and disassembly (IBMX) as measured by qRT–PCR. Relative abundance for each gene was determined by the $2^{-\Delta\Delta Ct}$ method. Fold change and standard error were log transformed for graphical representation. Changes in relative mRNA abundance for time points 30, 60, and 90 min after stimulation, standardized to untreated cells, were determined for (A) ICL1, (B) light-harvesting protein of PSI (Lhca2), (C) light-harvesting protein of PSI (Lhca5), and (D) minor chlorophyll a-b binding protein of PSII (Lhcb5/CP26).

networks on the basis of similar expression profiles (DERISI *et al.* 1997). The product of the FAP12 gene may therefore serve a structural role, whereas the products of FAP277 and -280 may play regulatory roles, perhaps in regulating flagellar length.

Among the genes that we identified as associated with flagellar assembly and disassembly are several linked to ciliary disease. For example, the ARFA1a gene showed a unique expression profile in *C. reinhardtii* during flagellar length changes. Other ARF family members have previously been linked to human ciliary disease. *Scorpion*, a zebrafish cystic kidney gene, is a small GTPase in the ARF family (PAZOUR *et al.* 2005) necessary for ciliary assembly (SUN *et al.* 2004). In addition, *C. elegans* ARL6, a member of the ARF-like (ARL) family of GTPases, is linked directly to Bardet–Beidl syndrome (FAN *et al.* 2004). ARL6 is specifically expressed in ciliated cells and undergoes bidirectional IFT (FAN *et al.* 2004). On the basis of the link between ARL6 and IFT, FAN *et al.* (2004) proposed a role in trafficking not only in the cytosol but also in the axoneme. The regulation of ARF expression that we found supports the possibility that ARF plays a similar role in *C. reinhardtii* IFT.

The expression profiles presented here demonstrate regulation of genes relating to information storage/processing and various types of metabolism, functions not normally associated with flagellar structure. These expression profiles yield clues to a molecular basis for the whole-cell response to stimulus-induced changes. The fact that only 21 of the 118 strongly regulated genes reported here are found in the flagellar proteome suggests that this whole-cell response is larger than previously recognized. For example, the expression profile that we constructed revealed upregulation of mRNAs encoding ICL1, a key enzyme in the glyoxylate pathway, and downregulation of mRNAs encoding the LHC components. Others (ZHANG *et al.* 2004; STOLC *et al.* 2005; MOSELEY *et al.* 2006) have also noted the decrease in relative abundance of LHC genes in response to various stimuli. PETRIDOU *et al.* (1997) showed that the relative abundance of ICL transcripts decreases within 30 min of exposure to light, suggesting a switch from stored energy (glyoxylate pathway) to photosynthetic energy use. We found a similar inverse relationship between the mRNA abundance of ICL and photosynthetic components in response to external stimuli. Cells may therefore switch to a stored form of energy while recovering from stimulation.

Our study characterizes known flagellar genes, flagellar-associated genes, and genes connected with the flagellum in ways not yet understood. This research begins to define the interrelationship between the cellular and molecular networks regulating flagellar length changes. Through global expression studies of the genes associated with flagellar assembly and disas-

sembly, we can begin to dissect the intricacies of this complex organelle and to uncover fundamental regulatory mechanisms that are part of a whole-cell response to stimulation.

The authors thank Amber Brown, Holly Sikes, Danielle Sherdan, and Andre Irsigler for advice and assistance. This work represents partial fulfillment of the requirements for the dissertation of K.L.C. It was supported by a Florida State University (FSU) Committee on Faculty Research Support grant to L.R.K. and an FSU dissertation grant to K.L.C.

LITERATURE CITED

Ainsworth, C., 2007 Cilia: tails of the unexpected. Nature **448:** 638–641.

Baker, E. J., J. A. Schloss and J. L. Rosenbaum, 1984 Rapid changes in tubulin RNA synthesis and stability induced by deflagellation in *Chlamydomonas*. J. Cell Biol. **99:** 2074–2081.

Bowtell, D., and J. Sambrook, 2003 *DNA Microarrays: A Molecular Cloning Manual*. Cold Spring Harbor Laboratory Press, Cold Spring Harbor, NY.

Brazelton, W. J., C. D. Amundsen, C. D. Silflow and P. A. Lefebvre, 2001 The bld1 mutation identifies the *Chlamydomonas* osm-6 homolog as a gene required for flagellar assembly. Curr. Biol. **11:** 1591–1594.

Cheshire, J. L., and L. R. Keller, 1991 Uncoupling of *Chlamydomonas* flagellar gene expression and outgrowth from flagellar excision by manipulation of Ca^{2+}. J. Cell Biol. **115:** 1651–1659.

Cheshire, J. L., J. H. Evans and L. R. Keller, 1994 Ca^{2+} signaling in the *Chlamydomonas* flagellar regeneration system: cellular and molecular responses. J. Cell Sci. **107:** 2491–2498.

Christensen, S. T., L. B. Pedersen, L. Schneider and P. Satir, 2007 Sensory cilia and integration of signal transduction in human health and disease. Traffic **8:** 97–109.

Curry, A. M., B. D. Williams and J. L. Rosenbaum, 1992 Sequence analysis reveals homology between two proteins of the flagellar radial spoke. Mol. Cell. Biol. **12:** 3967–3977.

Davenport, J. R., and B. K. Yoder, 2005 An incredible decade for the primary cilium: a look at a once-forgotten organelle. Am. J. Physiol. Renal Physiol. **289:** F1159–F1169.

Deane, J. A., D. G. Cole, E. S. Seeley, D. R. Diener and J. L. Rosenbaum, 2001 Localization of intraflagellar transport protein IFT52 identifies basal body transitional fibers as the docking site for IFT particles. Curr. Biol. **11:** 1586–1590.

DeRisi, J. L., V. R. Iyer and P. O. Brown, 1997 Exploring the metabolic and genetic control of gene expression on a genomic scale. Science **278:** 680–686.

Diener, D. R., L. H. Ang and J. L. Rosenbaum, 1993 Assembly of flagellar radial spoke proteins in *Chlamydomonas*: identification of the axoneme binding domain of radial spoke protein 3. J. Cell Biol. **123:** 183–190.

Elrad, D., and A. R. Grossman, 2004 A genome's-eye view of the light-harvesting polypeptides of *Chlamydomonas reinhardtii*. Curr. Genet. **45:** 61–75.

Evans, J. H., and L. R. Keller, 1997 Calcium influx signals normal flagellar RNA induction following acid shock of *Chlamydomonas reinhardtii*. Plant Mol. Biol. **33:** 467–481.

Fan, Y., M. A. Esmail, S. J. Ansley, O. E. Blacque, K. Boroevich *et al.*, 2004 Mutations in a member of the Ras superfamily of small GTP-binding proteins causes Bardet-Biedl syndrome. Nat. Genet. **36:** 989–993.

Hegde, P., R. Qi, K. Abernathy, C. Gay, S. Dharap *et al.*, 2000 A concise guide to cDNA microarray analysis. BioTechniques **29:** 548–556.

Keller, L. R., J. A. Schloss, C. D. Silflow and J. L. Rosenbaum, 1984 Transcription of α- and β-tubulin genes in isolated *Chlamydomonas* nuclei. J. Cell Biol. **98:** 1138–1143.

Lefebvre, P. A., S. A. Nordstrom, J. E. Moulder and J. L. Rosenbaum, 1978 Flagellar elongation and shortening in *Chlamydomonas*. IV. Effects of flagellar detachment, regeneration, and resorption on the induction of flagellar protein synthesis. J. Cell Biol. **78:** 8–27.

Lefebvre, P. A., C. D. Silflow, E. D. Wieben and J. L. Rosenbaum, 1980 Increased levels of mRNAs for tubulin and other flagellar proteins after amputation or shortening of *Chlamydomonas* flagella. Cell **20:** 469–477.

Li, J. B., J. M. Gerdes, C. Haycraft, Y. Fan, T. M. Teslovich *et al.*, 2004 Comparative genomics identifies a flagellar and basal body proteome that includes the BBS5 human disease gene. Cell **117:** 541–552.

Livak, K. J., and T. D. Schmittgen, 2001 Analysis of relative gene expression data using real-time quantitative PCR and the $2^{-\Delta\Delta C_t}$ method. Methods **25:** 402–408.

Luck, D., G. Piperno, Z. Ramanis and B. Huang, 1977 Flagellar mutants of *Chlamydomonas*: studies of radial spoke-defective strains by dikaryon and revertant analysis. Proc. Natl. Acad. Sci. USA **74:** 3456–3460.

Majumder, A. L., A. Chatterjee, K. Ghosh Dastidar and M. Majee, 2003 Diversification and evolution of L-myo-inositol 1-phosphate synthase. FEBS Lett. **553:** 3–10.

Marshall, W. F., and J. L. Rosenbaum, 2001 Intraflagellar transport balances continuous turnover of outer doublet microtubules: implications for flagellar length control. J. Cell Biol. **155:** 405–414.

Marshall, W. F., H. Qin, M. R. Brenni and J. L. Rosenbaum, 2005 Flagellar length control system: testing a simple model based on intraflagellar transport and turnover. Mol. Biol. Cell **16:** 270–278.

Michalak, M., R. E. Milner, K. Burns and M. Opas, 1992 Calreticulin. Biochem. J. **285:** 681–692.

Minagawa, J., K. C. Han, N. Dohmae, K. Takio and Y. Inoue, 2001 Molecular characterization and gene expression of lhcb5 gene encoding CP26 in the light-harvesting complex II of *Chlamydomonas reinhardtii*. Plant Mol. Biol. **46:** 277–287.

Moseley, J. L., C. W. Chang and A. R. Grossman, 2006 Genome-based approaches to understanding phosphorus deprivation responses and PSR1 control in *Chlamydomonas reinhardtii*. Eukaryot. Cell **5:** 26–44.

Nie, Z., and P. A. Randazzo, 2006 Arf GAPs and membrane traffic. J. Cell Sci. **119:** 1203–1211.

Pan, J., Q. Wang and W. J. Snell, 2004 An aurora kinase is essential for flagellar disassembly in *Chlamydomonas*. Dev. Cell **6:** 445–451.

Pan, J., Q. Wang and W. J. Snell, 2005 Cilium-generated signaling and cilia-related disorders. Lab. Invest. **85:** 452–463.

Pazour, G. J., B. L. Dickert, Y. Vucica, E. S. Seeley, J. L. Rosenbaum *et al.*, 2000 *Chlamydomonas* IFT88 and its mouse homologue, polycystic kidney disease gene Tg737, are required for assembly of cilia and flagella. J. Cell Biol. **151:** 709–718.

Pazour, G. J., N. Agrin, J. Leszyk and G. B. Witman, 2005 Proteomic analysis of a eukaryotic cilium. J. Cell Biol. **170:** 103–113.

Petridou, S., K. Foster and K. Kindle, 1997 Light induces accumulation of isocitrate lyase mRNA in a carotenoid-deficient mutant of *Chlamydomonas reinhardtii*. Plant Mol. Biol. **33:** 381–392.

Rosenbaum, J. L., J. E. Moulder and D. L. Ringo, 1969 Flagellar elongation and shortening in *Chlamydomonas*: the use of cycloheximide and colchicine to study the synthesis and assembly of flagellar proteins. J. Cell Biol. **41:** 600–619.

Sager, R., and S. Granick, 1953 Nutritional studies with *Chlamydomonas reinhardtii*. Ann. NY Acad. Sci. **56:** 831–838.

Schloss, J. A., 1990 A *Chlamydomonas* gene encodes a G protein β subunit-like polypeptide. Mol. Gen. Genet. **221:** 443–452.

Schloss, J. A., C. D. Silflow and J. L. Rosenbaum, 1984 mRNA abundance changes during flagellar regeneration in *Chlamydomonas reinhardtii*. Mol. Cell. Biol. **4:** 424–434.

Scholey, J. M., 2003 Intraflagellar transport. Annu. Rev. Cell Dev. Biol. **19:** 423–443.

Silflow, C. D., P. A. Lefebvre, T. W. McKeithan, J. A. Schloss, L. R. Keller *et al.*, 1982 Expression of flagellar protein genes during flagellar regeneration in *Chlamydomonas*. Cold Spring Harb. Symp. Quant. Biol. **46:** 157–169.

Silflow, C. D., R. L. Chisholm, T. W. Conner and L. P. Ranum, 1985 The two alpha-tubulin genes of *Chlamydomonas reinhardi* code for slightly different proteins. Mol. Cell. Biol. **5:** 2389–2398.

Stolc, V., M. P. Samanta, W. Tongprasit and W. F. Marshall, 2005 Genome-wide transcriptional analysis of flagellar regener-

ation in *Chlamydomonas reinhardtii* identifies orthologs of ciliary disease genes. Proc. Natl. Acad. Sci. USA **102:** 3703–3707.

Sun, Z., A. Amsterdam, G. J. Pazour, D. G. Cole, M. S. Miller *et al.*, 2004 A genetic screen in zebrafish identifies cilia genes as a principal cause of cystic kidney. Development **131:** 4085–4093.

Williams, B. D., D. R. Mitchell and J. L. Rosenbaum, 1986 Molecular cloning and expression of flagellar radial spoke and dynein genes of *Chlamydomonas*. J. Cell Biol. **103:** 1–11.

Williams, B. D., M. A. Velleca, A. M. Curry and J. L. Rosenbaum, 1989 Molecular cloning and sequence analysis of the *Chlamydomonas* gene coding for radial spoke protein 3: flagellar mutation pf-14 is an ochre allele. J. Cell Biol. **109:** 235–245.

Witman, G. B., K. Carlson, J. Berliner and J. L. Rosenbaum, 1972 *Chlamydomonas* flagella: I. Isolation and electrophoretic analysis of microtubules, matrix, membranes, and mastigonemes. J. Cell Biol. **54:** 507–539.

Yang, P., D. R. Diener, C. Yang, T. Kohno, G. J. Pazour *et al.*, 2006 Radial spoke proteins of *Chlamydomonas* flagella. J. Cell Sci. **119:** 1165–1174.

Yang, Y. H., and T. Speed, 2002 Design issues for cDNA microarray experiments. Nat. Rev. Genet. **3:** 579–588.

Youngblom, J., J. A. Schloss and C. D. Silflow, 1984 The two beta-tubulin genes of *Chlamydomonas reinhardtii* code for identical proteins. Mol. Cell. Biol. **4:** 2686–2696.

Yue, H., P. S. Eastman, B. B. Wang, J. Minor, M. H. Doctolero *et al.*, 2001 An evaluation of the performance of cDNA microarrays for detecting changes in global mRNA expression. Nucleic Acids Res. **29:** E41.

Zhang, Z., J. Shrager, M. Jain, C. W. Chang, O. Vallon *et al.*, 2004 Insights into the survival of *Chlamydomonas reinhardtii* during sulfur starvation based on microarray analysis of gene expression. Eukaryot. Cell **3:** 1331–1348.

Communicating editor: S. Dutcher